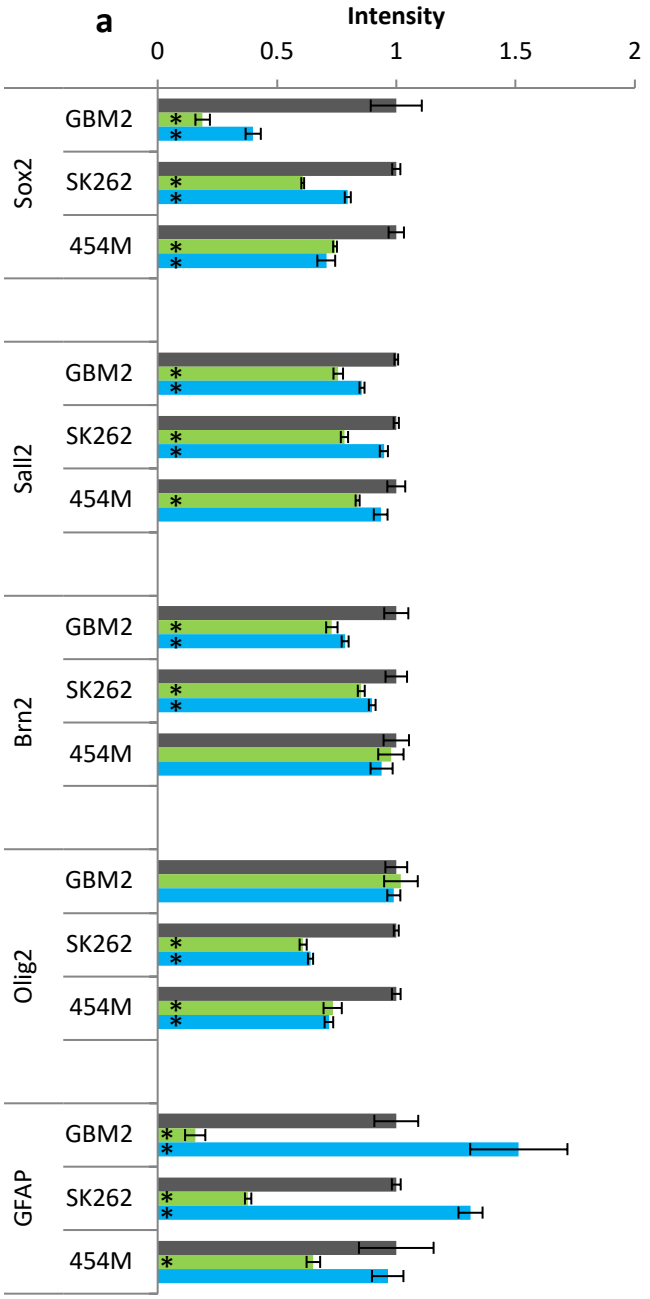

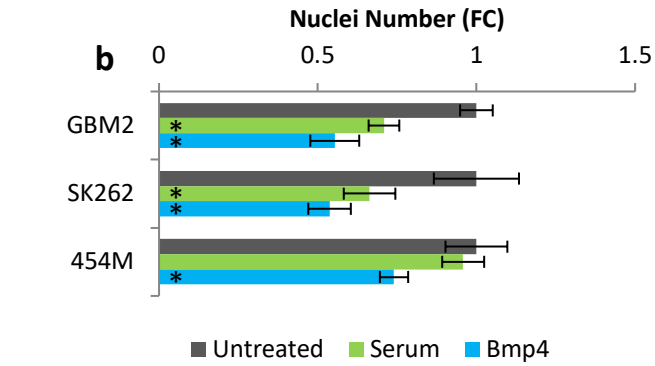

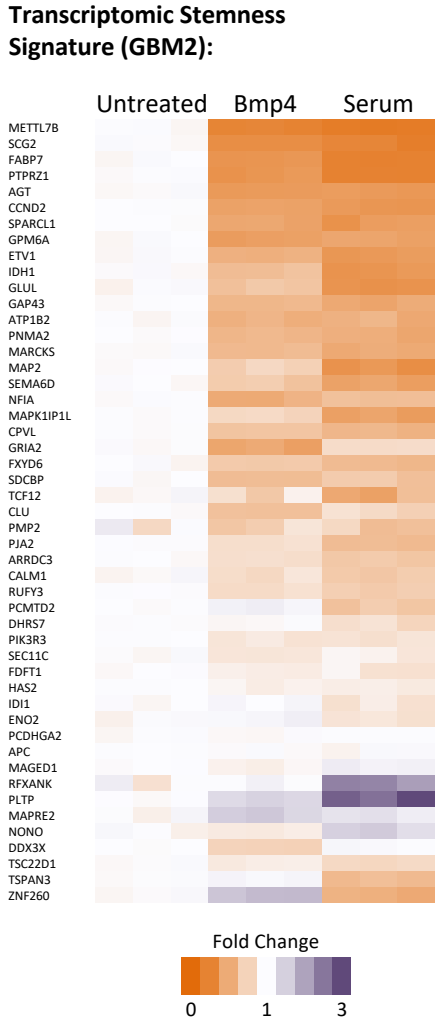

Supplementary Figure 1.

Supplementary Figure 1.

(a) Fold change in immunofluorescence intensity for Sox2, Sall2, Brn2, Olig2 and GFAP for 3 days serum or Bmp4 treated primary human GBM lines compared to untreated cells (mean ± S.D, n=3, *p<0.05, unpaired two-tailed t-test).

(b) Fold change in nuclei number of 3 days serum or Bmp4 treated primary human GBM lines compared to untreated cells (mean ± S.D, n=3, *p<0.05, unpaired two-tailed t-test).

(c) Heat map showing expression changes of genes identified as TPC stemness signature(23) in GBM2 cells following 3 days treatment with either serum or Bmp4 (values shown as fold change: FPKM value in every sample divided by average FPKM value of the 3 untreated samples).

Category	GO Term	Description	Fold Enrichment	P-value
Neurogenesis	GO:0022008	neurogenesis	1.41	1.4E-20
	GO:0050767	regulation of neurogenesis	1.46	1.1E-10
	GO:0050769	positive regulation of neurogenesis	1.5	3.5E-06
	GO:0050768	negative regulation of neurogenesis	1.47	2.8E-02
Cell Cycle	GO:0007049	cell cycle	1.43	1.7E-20
	GO:0022402	cell cycle process	1.48	3.2E-18
	GO:0044770	cell cycle phase transition	1.67	1.9E-07
	GO:0044839	cell cycle G2/M phase transition	1.75	7.4E-04
Neuronal Differentiation	GO:0045595	regulation of cell differentiation	1.36	1.9E-16
	GO:0045664	regulation of neuron differentiation	1.49	1.8E-09
	GO:0045666	positive regulation of neuron differentiation	1.54	1.4E-05
Migration	GO:0030334	regulation of cell migration	1.45	3.7E-10
	GO:0030335	positive regulation of cell migration	1.42	4.3E-04
	GO:0030336	negative regulation of cell migration	1.52	1.1E-02
Neuron Projection	GO:0031175	neuron projection development	1.47	1.1E-09
	GO:0048858	cell projection morphogenesis	1.55	3.9E-09
	GO:0031344	regulation of cell projection organization	1.48	4.2E-09
	GO:0048812	neuron projection morphogenesis	1.54	8.6E-09
	GO:0010975	regulation of neuron projection development	1.5	1.7E-06
	GO:0050770	regulation of axonogenesis	1.7	8.4E-04
Morphogenesis	GO:0000904	cell morphogenesis involved in differentiation	1.52	2.9E-09
	GO:0010769	regulation of cell morphogenesis involved in differentiation	1.68	2.2E-07
	GO:0048667	cell morphogenesis involved in neuron differentiation	1.53	3.8E-07
	GO:0010770	positive regulation of cell morphogenesis involved in differentiation	1.68	1.3E-02
Wnt Pathway	GO:0030111	regulation of Wnt signaling pathway	1.59	1.4E-06
	GO:0060828	regulation of canonical Wnt signaling pathway	1.63	1.4E-05
	GO:0016055	Wnt signaling pathway	1.5	5.7E-05
	GO:0090090	negative regulation of canonical Wnt signaling pathway	1.73	1.2E-04
Chromatin Organization	GO:0006325	chromatin organization	1.33	5.0E-04
	GO:0016570	histone modification	1.39	3.2E-02

Supplementary Figure 2.

Supplementary Figure 2.

GO terms enriched by serum and Bmp4 treatments and identified using PANTHER v11(47).

	Controls	Sox2 (% efficacy)	GFAP (% efficacy)	Viable (z-score)	Piknotic (z-score)
	DMSO	5.06	-0.40	0.06	0.23
	Bmp4	100.39	106.70	-2.33	1.20
Decrease SOX2 & Increase GFAP	Amlodipine	114.11	42.57	-6.51	2.70
	Mebendazole	110.34	52.00	-6.17	13.49
	Vanoxerine	102.79	104.90	-6.17	8.77
	Sertindole	81.63	73.30	-7.34	4.72
	Carvedilol	66.05	53.91	-6.32	1.35
	Fendiline	64.00	69.36	-6.36	2.02
	Trifluoperazine	51.09	103.48	-3.42	4.72
	Paroxetine	44.51	135.75	-4.90	4.72
	Fenbendazole	43.47	98.84	-6.14	7.42
Decrease SOX2	Lanatoside C	179.74	-41.22	-4.40	3.37
	Doxorubicin	169.50	-23.69	-6.61	-1.35
	Proscillaridin	154.27	-28.93	-6.02	-0.67
	Digoxin	145.72	-33.41	-5.88	0.67
	Methazolamide	139.27	-43.02	-6.07	2.70
	Nocodazole	136.68	-30.83	-5.77	11.47
	Digitoxigenin	130.67	-41.17	-5.90	0.67
	Podophyllotoxin	129.92	-43.33	-4.73	12.14
	Thiostrepton	114.66	-48.19	-6.59	2.70
	Colchicine	111.76	-42.65	-5.98	7.42
	Althiazide	90.89	-45.17	-3.76	2.70

Supplementary Figure 3.

Supplementary Figure 3.

Candidate compounds identified in the Prestwick library screen using SOX2 and GFAP readouts (Fig.1a); shown are % of Sox2 efficacy (inhibition), % of GFAP efficacy (activation), robust z-scores of viable and pyknotic cell counts.

a

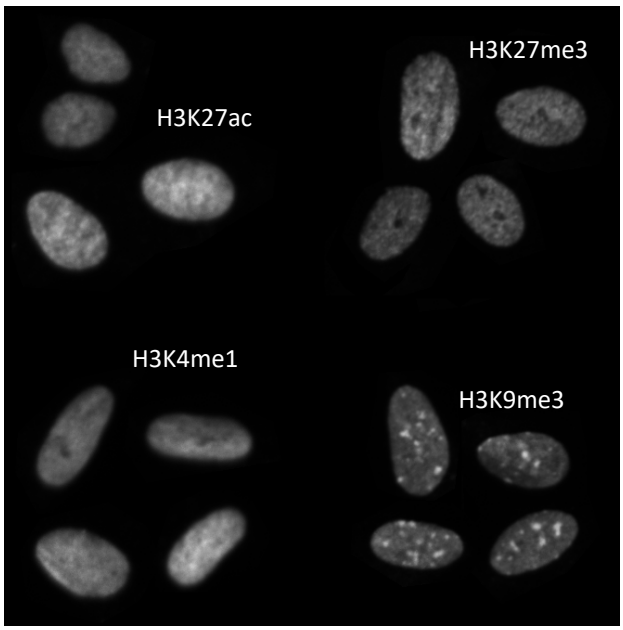

b

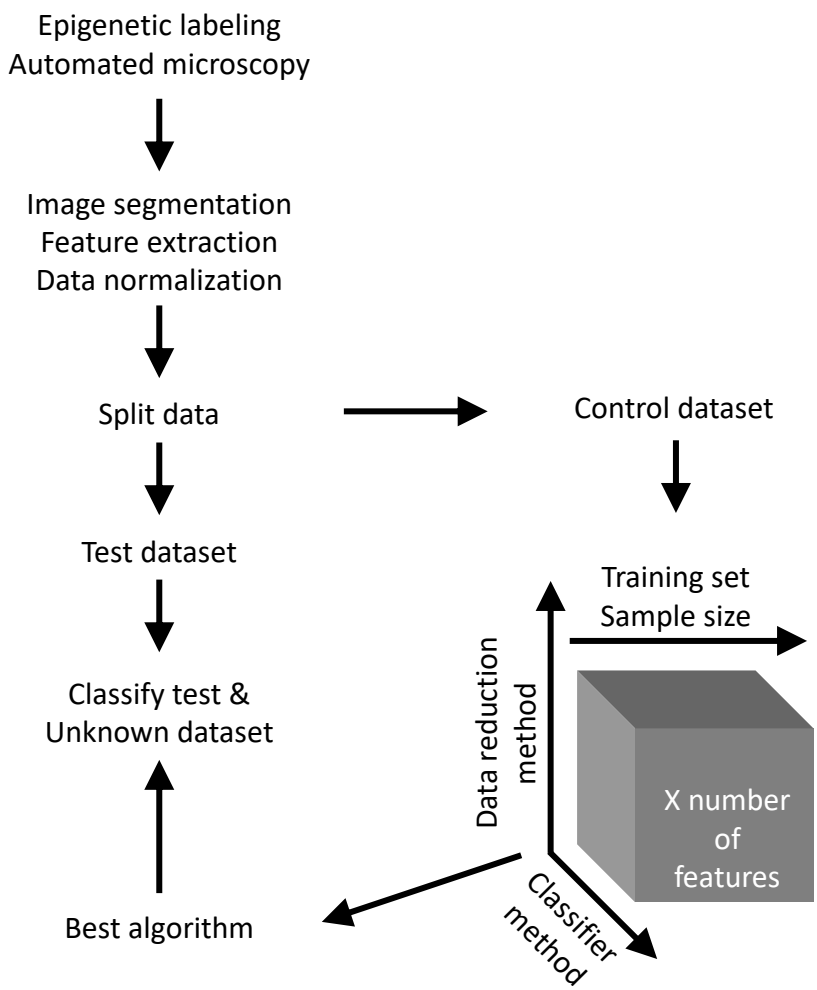

Supplementary Figure 4.

Supplementary Figure 4.

(a) Images showing H3K27ac, H3K27me3, H3K4me1 and H3K9me3 specific immunofluorescent labeling in the untreated GBM2 cells.

(b) MIEL-SVM classification pipeline. Nuclei were immunostained for various histone or DNA modifications then imaged using automated fluorescent microscopy and the micrographs were processed using batch analysis. Nuclei were identified and segmented using Hoechst, features were calculated for each nucleus individually based on patterns of histone modifications, and the data were imported into the miClassify script(26). For SVM classification, each cell population was split into training and test sets. The script runs multiple iterations each with different randomly selected sets of images for training and scoring to identify the features from the training data that consistently yield the most accurate SVM classifier. The optimized feature set is used to train and optimize an SVM which is then used to classify the test data.

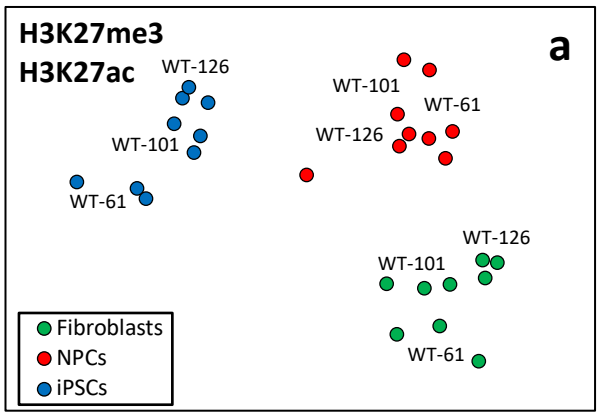

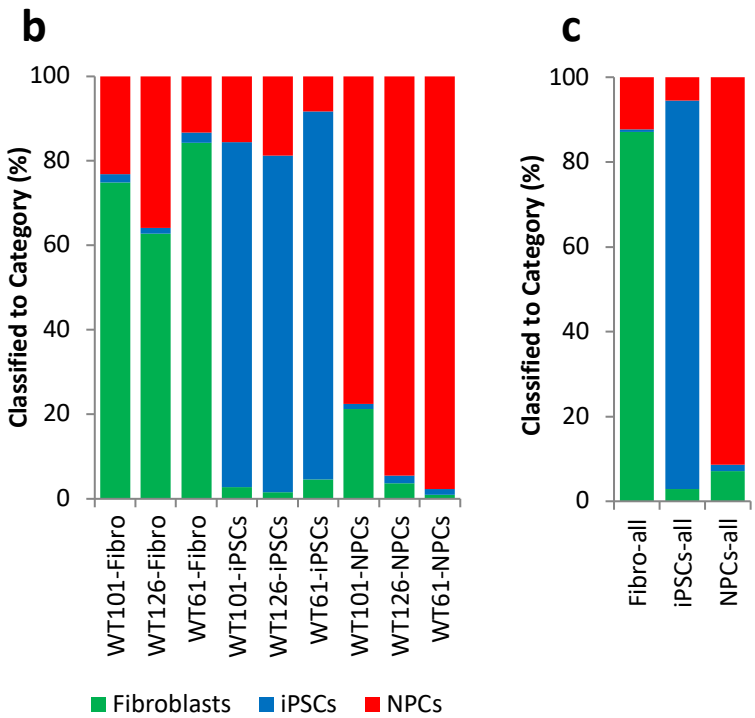

d

		Fibroblasts		iPSCs		NPCs	
		WT-101	WT-126	WT-101	WT-126	WT-101	WT-126
Fibro-blasts	WT-61	75%	81%				
	WT-101		67%				
iPSCs	WT-61			65%	84%		
	WT-101				77%		
NPCs	WT-61					76%	68%
	WT-101						76%

Supplementary Figure 5.

Supplementary Figure 5.

Fibroblast, iPSC and NPC cell lines from 3 human donors (WT-61, WT-101 and WT-126); texture features based on H3K27ac and H3K27me3 marks.

(a) Distance map depicting the relative Euclidean distance between the multiparametric centroids of the 9 cell lines. Each of the 9 cell lines was processed in triplicates shown on the map.

(b, c) Three-way classifications of (b) the 9 cell lines using an SVM classifier trained on fibroblast, iPSCs, and NPCs, from WT-61 donor; (overall correct categorization in 9 lines was 83%) and (c) pooled cell lines using an SVM classifier trained on pooled fibroblast, iPSCs, and NPCs (overall correct categorization in 9 lines was 90%).

(d) Accuracy of pairwise SVM classification of the fibroblast, iPSCs, and NPCs derived from 3 human donors (WT-61, WT-101 and WT-126), using H3K9me3 and H3K4me1 texture features.

a

Lin-
c-kit+
Sca1+

FACS

Mac1+
GR1+

B220+

CD3+

B cells

T cells

Macrophages

LT-HSC
Slamf1+
Flk2-

ST-HSC
Slamf1-
Flk2-

MPP
Slamf1-
Flk2+

b

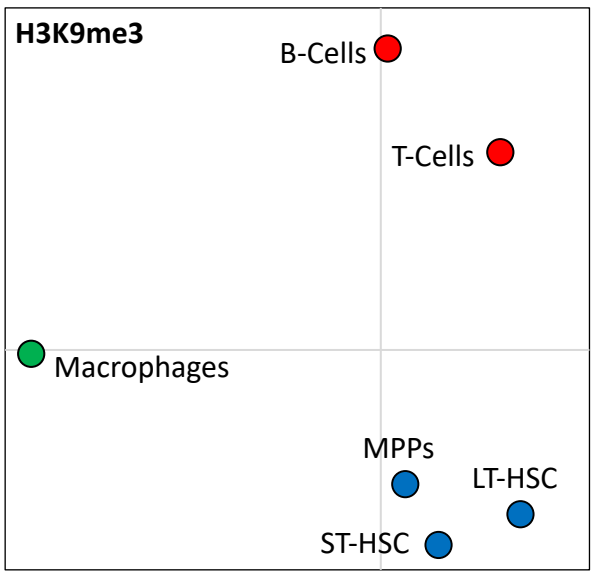

c

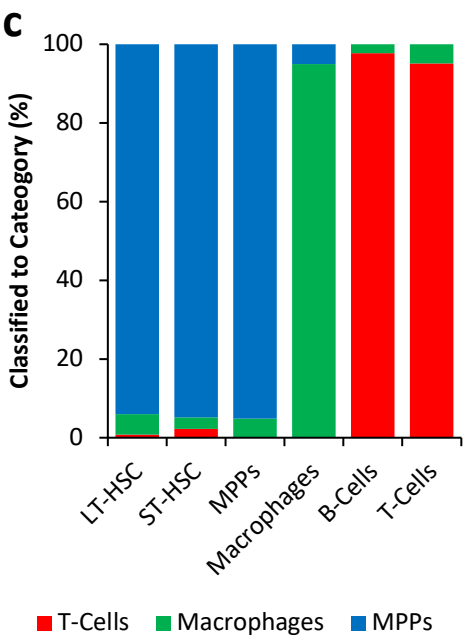

d

	T-Cells (CD3)	B-Cells (B220)	Macrophages	ST-HSC	MPPs	LT-HSC
T-Cells (CD3)		75%	99%	98%	100%	99%
B-Cells (B220)			100%	100%	98%	99%
Macrophages				96%	98%	97%
ST-HSC					67%	67%
MPPs						68%
LT-HSC						

Supplementary Figure 6.

Supplementary Figure 6.

(a) Surface markers for isolation of hematopoietic cells by flow cytometry.

(b) Distance map depicting the relative Euclidean distance between the multiparametric centroids of image texture features from immunofluorescence micrographs of 6 hematopoietic cell types.

(c) Three-way classification of hematopoietic stem/progenitor cells, T and B lymphoid cells and macrophages – using an SVM classifier trained on randomly selected sub-sets of MPPs, macrophages and T-cells.

(d) Accuracy of pairwise SVM classification between the 6 hematopoietic cell types.

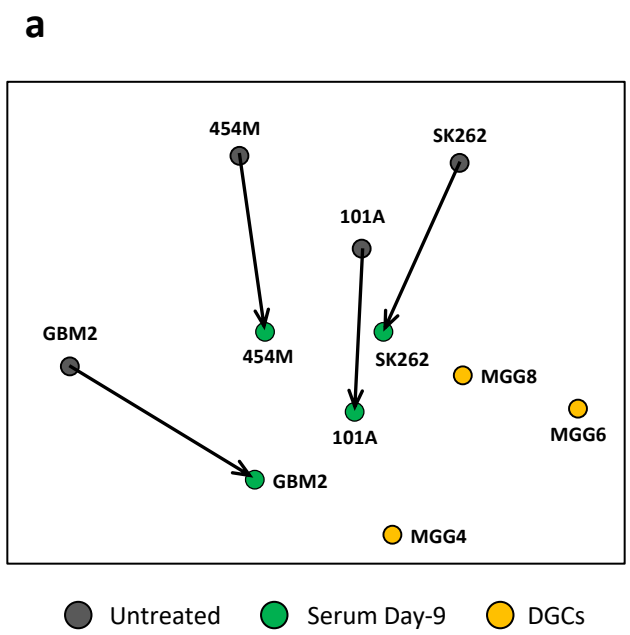

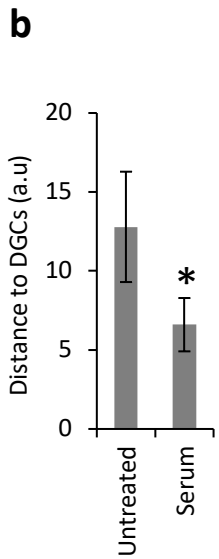

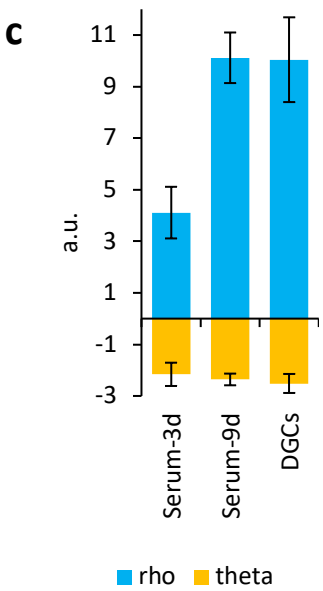

Supplementary Figure 7.

Supplementary Figure 7.

(a, b) Euclidean distances between multiparametric centroids of image texture features based on H3K27ac and H3K27me3 marks of 4 untreated or 9 days serum treated primary GBM lines and 3 reference MGG-DGC lines. (b) Mean ± S.D, $p<0.05$, n=4 GBM lines, unpaired two-tailed t-test.

(c) Average rho and theta values for cells and treatments in Fig. 3d.

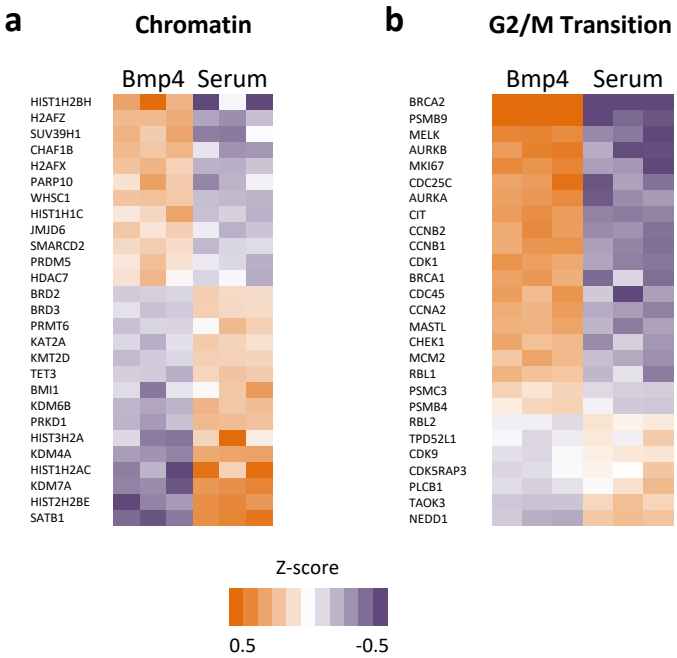

Supplementary Figure 8.

Supplementary Figure 8.

(a, b) Heat maps showing differential expression of selected genes from the GO term (a) chromatin-modification (GO:0006325) or (b) cell-cycle G2/M phase transition (GO:0044839). Expression levels (FPKM) are represented as z-score to highlight difference in levels of expression.

a

Compound	Category	Classified to Treatment	Normalized Distance
Digoxigenin	Na/K-ATPase	0.67	0.93
Digoxin	Na/K-ATPase	0.51	0.94
Digitoxigenin	Na/K-ATPase	0.61	0.95
Lanatoside C	Na/K-ATPase	0.71	0.96
Fenbendazole	Microtubules	0.90	0.59
Mebendazole	Microtubules	0.91	0.74
Flubendazol	Microtubules	0.72	0.85
Etoposide	Topoisomerase	0.82	0.43
Irinotecan	Topoisomerase	0.97	0.56
Topotecan	Topoisomerase	0.98	0.79
Cytarabine	Nucleotide	0.94	0.46
Trifluridine	Nucleotide	0.71	0.79
Floxuridine	Nucleotide	0.65	0.92
Gemcitabine	Nucleotide	0.95	0.95
Cladribine	Nucleotide	0.94	0.99
Oxyphenbutazone	NSAID	0.74	0.58
Haloprogin	antifungal	0.69	0.60
Thiostrepton	antibiotic	0.92	0.85
Hycanthone	schistosomicide	0.72	0.89
Methiazole	Thyroperoxidase	0.84	0.99

b

	uM	Classified as: Base	Treated
Untreated		77.1%	22.9%
Serum		31.2%	68.8%
Bmp4		33.8%	66.2%
Fenbendazole	0.3	83.4%	16.6%
	1	45.3%	54.7%
	3	26.4%	73.6%
Mebendazole	0.3	78.5%	21.5%
	1	23.5%	76.5%
	3	21.9%	78.1%
Cytarabine	0.3	43.9%	56.1%
	1	26.3%	73.7%
	3	16.6%	83.4%
Trifluridine	0.3	69.8%	30.2%
	1	64.8%	35.2%
	3	38.1%	61.9%
Irinotecan	0.3	75.4%	24.6%
	1	36.3%	63.7%
	3	16.2%	83.8%
Etoposide	0.3	41.3%	58.7%
	1	24.4%	75.6%
	3	19.7%	80.3%
Digitoxigenin	0.3	46.9%	53.1%
	1	32.8%	67.2%
	3	39.0%	61.0%
Digoxin	0.3	36.9%	63.1%
	1	38.0%	62.0%
	3	35.8%	64.2%

Supplementary Figure 9.

Supplementary Figure 9.

(a) Twenty hit compounds grouped by the functional classes. For the pairwise classification, the classifier was trained on texture features derived from H3K27ac and H3K27me3 images of serum- or Bmp4-treated GBM2 (vs untreated; cut off = classified to treatment>50%). Normalized distance calculated as the Euclidean distance of a compound to either serum or Bmp4 (the smaller of the two) divided by the distance of untreated cells to the same control (cutoff = normalized distance<1).

(b) Table showing pairwise classification of indicated drug-treated GBM2 using a classifier trained on texture features derived from H3K27ac and H3K27me3 images of DMSO- and either serum- or Bmp4-treated GBM2 cells.

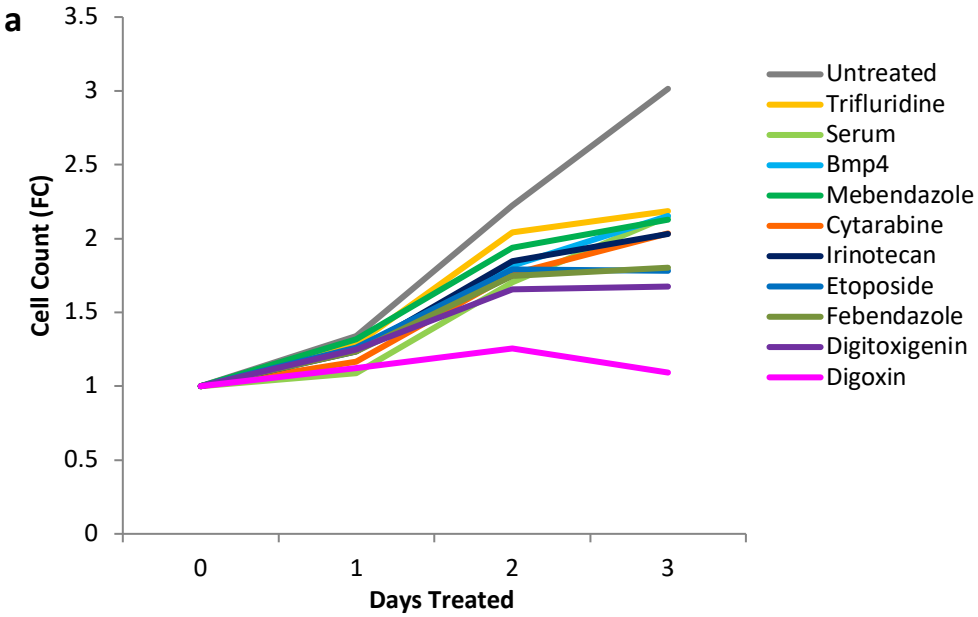

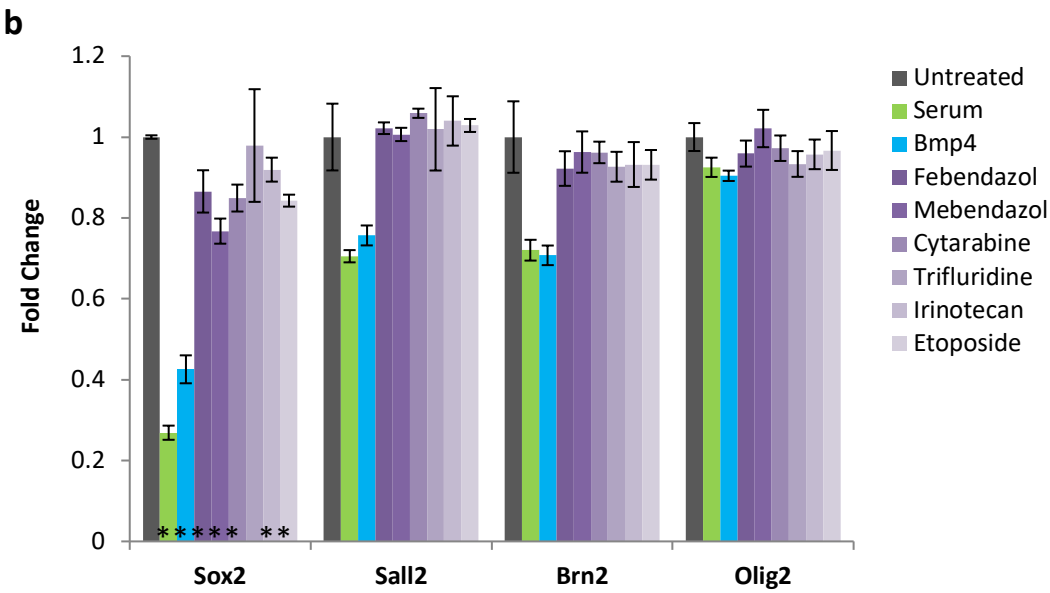

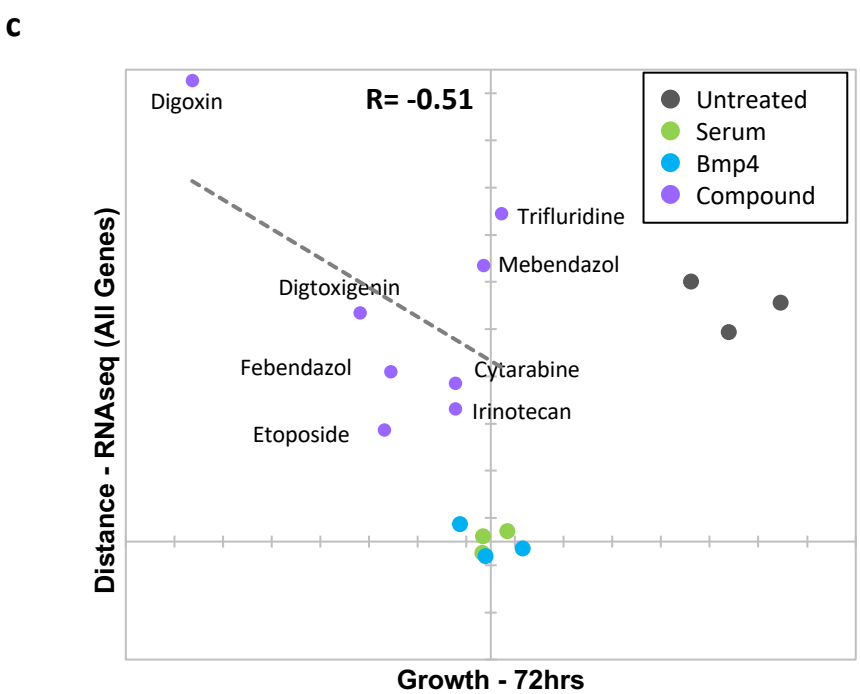

Supplementary Figure 10.

Supplementary Figure 10.

(a) Growth dynamics (fold change in cell count – vertical axis) of untreated, serum-, Bmp4- or drug-treated GBM2 cells over 3 days.

(b) Fold change in Sox2, Sall2, Brn2, and Olig2 immunofluorescence intensity of untreated or serum-, Bmp4- or drug-treated GBM2 cells; 3 days of treatment (mean ± S.D, n=3, $p<0.05$, unpaired two-tailed t-test).

(c) Scatter plot showing the correlation of gene expression profile-based ranking and growth rates for untreated, serum-, Bmp4-, or 8 drugs-treated GBM2 cells. Euclidean distance to serum or Bmp4 treated GBM2 cells was calculated using transcriptomic profiles (vertical axis), or growth rate after 72 hours treatment with immunofluorescence intensity (horizontal axis). Distances and growth rates were normalized to untreated and serum/Bmp4 treated GBM2 cells. R denotes Pearson correlation coefficient.